BLAST PERFORMANCE AND RESPONSE LIMITS OF NON-LOAD BEARING CONCRETE PANELS

Thomas J. Mander, P.E., Baker Engineering and Risk Consultants, Inc., San Antonio, TX
Michael A. Polcyn, Baker Engineering and Risk Consultants, Inc., San Antonio, TX

ABSTRACT

A series of ten full-scale precast concrete panels were tested with blast loads generated from a shock tube. Specimens had a range of panel thicknesses, span lengths, flexural reinforcement ratios, and shear stirrup spacing. All panels had simple bearing connections without in-plane restraint. Panels were tested multiple times to define support rotations at which different levels of damage occurred. The experimental data demonstrated that the members' material and geometric properties altered the onset of various levels of damage. Panels remained substantially intact at observed support rotations that exceeded the prescribed crushing and failure limits defined for the panels tested.

Non-linear single degree of freedom analyses of the experiments are presented in this paper. Comparisons are made using customary elastic-plastic resistance functions, as well as multi-linear resistance functions, accounting for the constitutive properties of plain concrete and reinforcing steel. The multi-linear model used Takeda hysteresis to account for altering unloading and reloading stiffness during dynamic response. Peak and permanent displacements were predicted more accurately with this resistance function than with the common elastic-plastic approach. The robustness of the model was confirmed by adequately predicting deflections of panels that were loaded multiple times in the experimental study. This model can allow qualitative, rather than quantitative, response criteria to be satisfied, providing a more realistic expectation of damage for defined blast threats.

Keywords: Blast, Shock Tube, Concrete Panels, Response Criteria, Dynamic Analysis

INTRODUCTION

Precast reinforced concrete panels are frequently used as non-load bearing exterior walls for blast-resistant structures. They provide good thermal resistance against fire and penetration resistance against potential flying debris. Additionally, reinforced concrete panels have high inertial resistance to blast loading, and the desired level of strength can be achieved by modifying the reinforcement content.

Blast analysis and design of such panels is most commonly performed at a component level, using single-degree-of-freedom (SDOF) methods. The peak deflection and corresponding support rotation from the SDOF analysis are of key importance, and are compared to prescriptive limits to satisfy a level of component damage. The previously published limiting values have been derived from observed damage to components from blast tests and corresponding values of support rotations. One of the purposes of the testing used in this paper was to evaluate the accuracy of the existing criteria.

Response criteria are used universally for all components responding in flexure. The published limits are independent of factors such as flexural reinforcing ratios, span-to-depth ratios, support conditions, and material properties, all of which affect the ductility of reinforced concrete sections. The presence and extent of shear reinforcing is included as a factor in the criteria. Hence these prescriptive response criteria prevent blast engineers from accounting for geometric and material properties that affect the strength and ductility of reinforced concrete sections. The work reported herein introduces an improved method of analyzing reinforced concrete members subjected to blast loads. The overall objectives of this paper are to: (1) present the results of a series of blast tests on reinforced concrete panels in the BakerRisk shock tube; (2) compare the experimental results with response criteria; and (3) validate an improved analytical methodology for reinforced concrete members subject to blast loads.

Throughout this paper, the calculation of support rotation from deflection uses the idealization shown in Fig. 1, which assumes plastic response of a simply-supported beam or panel.

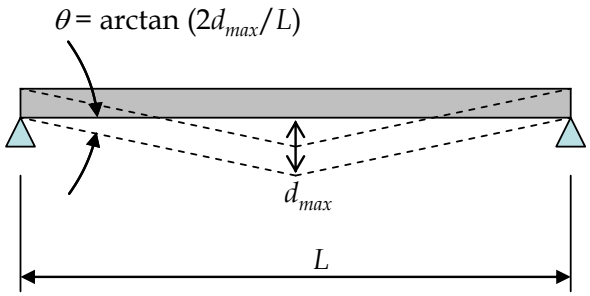

Fig. 1 Definition of Support Rotation as Function of Maximum Displacement

RESPONSE CRITERIA FOR BLAST DESIGN

The primary source of design guidance for conventionally loaded reinforced concrete wall panels is from ACI 318-08.[1] Similar design equations are provided for precast members in the PCI Design Handbook.[2] By contrast, no such universally applicable design guideline is used in the field of blast engineering. Various guidelines exist for explosive safety, anti-terrorism, and the chemical and processing industry. A component-level analysis using single-degree-of-freedom (SDOF) methods is accepted within each of these industries. However, quantitative values of support rotation and qualitative descriptions of these response limits generally differ between the various blast guidelines. The recently published document ASCE 59-11[3] provides a summary of the different response limits used in these industries.

The response limits referenced in ASCE 59-11 are from the U.S. Army Corps of Engineers (USACE) Protective Design Center (PDC) response criteria for SDOF components.[4,5] These limits were developed for Department of Defense (DoD) facilities designed against high explosive (HE) terrorist threats. Response criteria were developed from the Component Explosive Damage Assessment Workbook (CEDAW),[6] which considered three different HE test programs on reinforced concrete panels. Loads in these three test programs were mostly in the impulsive region (high pressure, short duration) of the panels tested[7,8,9] with peak support rotations ranging from 0.1° to 6.1°.

USACE criteria define four Levels of Protection (LOP) as: High (HLOP), Medium (MLOP), Low (LLOP) and Very Low (VLLOP). These LOPs respectively correspond to expected element damage denoted as Superficial, Moderate, Heavy and Hazardous. Quantitative response limits listed in Table 1 are divided into three component types. Single-reinforced panels and double-reinforced panels are given the same response criteria, provided the double-reinforced panels do not have shear reinforcement. Panels with double reinforcement and shear reinforcement (spaced along their span length no greater than half the effective member depth) are allowed higher levels of support rotation at the Moderate and Heavy damage levels. Note that all response criteria are independent of geometry, material properties, and reinforcement ratios, and are only intended to be used with SDOF analyses.

Table 1. Quantitative Response Limits (from PDC TR-06-08)

Component Type	Superficial		Moderate		Heavy		Hazardous	
	μ	θ	μ	θ	μ	θ	μ	θ
Single-reinforced panel	1	-	-	2°	-	5°	-	10°
Double-reinforced panel without shear reinforcement	1	-	-	2°	-	5°	-	10°
Double-reinforced panel with shear reinforcement	1	-	-	4°	-	6°	-	10°

Qualitative damage descriptions are provided by PDC TR-06-08 in a nonspecific manner, with the same qualitative descriptions (Table 2) used for all structural components (concrete, steel, masonry, etc.). In contrast, ASCE 59-11 published qualitative response limits specific to reinforced concrete beams and columns (Table 3). Since a distinction is not made between beams or panels in response criteria, these descriptions are assumed valid for reinforced concrete panels.

Table 2. Qualitative Response Limits for All Structural Components (from PDC TR-06-08)

PDC TR-06-08 Damage Level	Component Consequence
B1 (HLOP)	Superficial damage. Component has no visible damage.
B2 (MLOP)	Moderate damage. Component has some permanent deflection. It is generally repairable, if necessary, although replacement may be more economical and aesthetic
B3 (LLOP)	Heavy Damage. Component has not failed, but it has significant permanent deflections, causing it to be irreparable.
B4 (VLLOP)	Hazardous Failure. Component has failed, and debris velocities range from insignificant to very significant.
> B4	Blowout. Component is overwhelmed by the blast load causing debris with significant velocities.

Table 3. Qualitative Response Limits for Reinforced Concrete Beams (from ASCE 59-11)

Limit State	Superficial	Moderate	Heavy	Hazardous
Reinforcement	No damage	No damage	Local buckling of longitudinal reinforcement	Fracture of longitudinal and transverse reinforcement
Core concrete	No visible, permanent structural damage	Minor cracking (repairable by injection grouting)	Substantial damage	Rubble
Cover	No visible, permanent structural damage	Substantial spalling	Lost	Lost
Stability	None	None	Local buckling of longitudinal reinforcement	Global Buckling

ANALYSIS OF REINFORCED CONCRETE PANELS

Blast design guidelines specify that the ultimate (plastic) capacity of reinforced concrete sections be based upon static principles, albeit using assumed dynamic increase factors for concrete and steel. An elastic-plastic resistance function is employed in SDOF analyses for components responding in flexure. The peak dynamic deflection is of primary interest from

an SDOF analysis, and is converted to an equivalent support rotation, and compared to quantitative criteria (such as that in Table 1) using the equation shown earlier in Fig. 1. This method does not account for the actual state of stress or strain in the concrete and reinforcement when the panel reaches its maximum deflection. It is also unable to account for the additional ductility that a section may possess due to the rebar detailing.

Reinforced concrete members exhibit strain hardening in steel, softening in concrete, and additional softening under unloading. Hence an elastic–perfectly plastic modeling technique is not entirely appropriate, particularly at large deflections. A moment-curvature model including softening of concrete and strain hardening of reinforcing steel was developed as part of the current research. Unconfined and confined concrete stress-strain curves were based on existing analytical models that have been validated with experimental testing by other researchers.[10,11] Steel reinforcement was modeled using a power-law equation to generate a single equation that defines the entire stress-strain curve of reinforcing steel. Equation 1 allows the steel stress, f_s, to be determined for any given steel strain, ε_s.

$$f_s = \frac{E_s \varepsilon_s}{\left\{1 + \left|\frac{\varepsilon_s}{\varepsilon_{dy}}\right|^{20}\right\}^{0.05}} + \left(f_{du} - f_{dy}\right)\left|1 - \frac{|\varepsilon_{su} - \varepsilon_s|^p}{\{|\varepsilon_{su} - \varepsilon_{sh}|^{20p} + |\varepsilon_{su} - \varepsilon_s|^{20p}\}^{0.05}}\right| \qquad \textit{Equation 1}$$

$$\text{where } p = \frac{\varepsilon_{sh}(\varepsilon_{su} - \varepsilon_{sh})}{(f_{du} - f_{dy})}$$

The dynamic yield stress, f_{dy}, elastic modulus, E_s, dynamic yield strain, ε_{dy}, and ultimate stress, f_{du}, were calculated using the measured uniaxial tension test values (for the steel used in the panels), and multiplied by appropriate dynamic increase factors. The strains at the onset of strain hardening, ε_{sh}, and the ultimate strain, ε_{su} were based on published values for ASTM A615 reinforcement.[12]

Moment-curvature plots were converted to force-displacement curves assuming simple supports and neglecting shear deformations, using a previously published[13] and validated method. Plastic deflections are a function of the plastic hinge length, calculated as a function of the ratio of maximum moment to yield moment, rather than using an empirical relationship for an assumed plastic hinge length. Fig. 2(a) plots an example case for a 12 ft long panel with reinforcement-to-balanced steel ratio (ρ/ρ_b) equal to 0.2. The elastic-plastic function is shown to under-predict the peak resistance, which will influence support reaction predictions. The moment-curvature-based resistance function supports prediction of the deflections at which concrete cracking, strain hardening, crushing, and failure (not shown) occurs.

For SDOF analysis, elastic-plastic resistance functions use the same unloading stiffness as the initial elastic stiffness. The moment-curvature models developed used a modified Takeda[14] hysteretic model, which accounts for softening under unloading and reloading. This impacts the prediction of residual displacements and rebound (negative) reactions, as illustrated in Fig. 2(b).

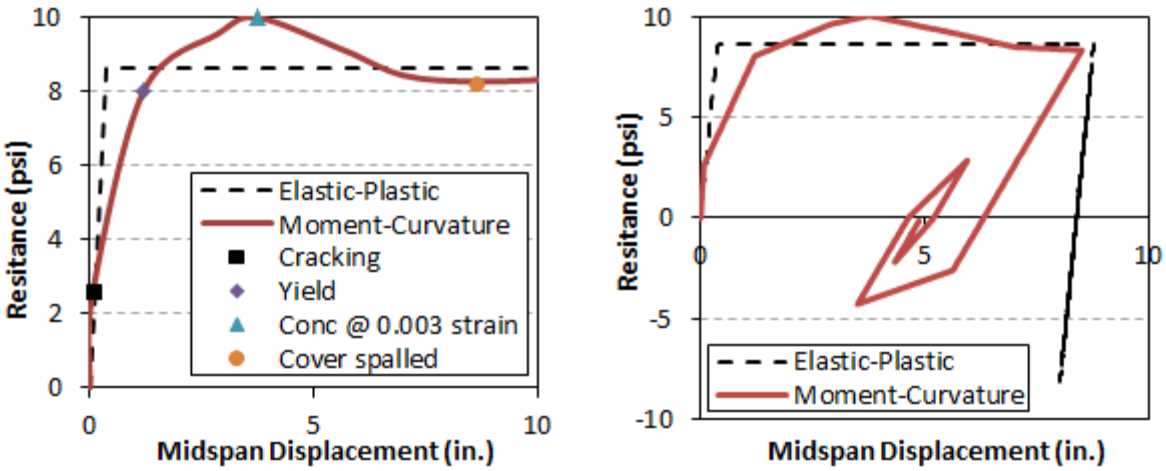

(a) Resistance Curves (b) SDOF Unloading

Fig. 2 Example Resistance-Displacement Curve

EXPERIMENTAL STUDY

Five different pairs of reinforced concrete panels with each panel denoted "A" or "B" were tested in the BakerRisk shock tube. The overall objective of the test program was to subject various concrete wall panel designs to Moderate and Heavy damage levels. Test article selection focused on three key parameters: longitudinal reinforcing ratios, span-to-depth ratios, and shear reinforcing content.

Table 4 presents the test matrix, along with details of these three parameters. Differences between "A" and "B" panels for the same test were usually in the shear steel details. Where used, shear steel consisted of a closed No. 3 hoop, and No. 3 stirrups on interior bars. Selection of the panel specimens was based on a parametric study completed using the moment-curvature analysis method, along with considerations of the shock tube's pressure and impulse capabilities.

All specimens were designed as full-scale panels, satisfying the minimum reinforcing and cover requirements of ACI 318-08. Spans and thicknesses were varied, but all panels were 48 inches wide. Steel reinforcing cages were constructed with ASTM A615 Grade 60 reinforcing steel. Additional bars were set aside for tensile testing, to characterize the yield and ultimate stresses for each bar size. Measured yield stresses for the primary reinforcing (i.e., not the #3 stirrups) are provided in Table 5, along with other material and dimensional data.

Cages were placed in wood forms, and concrete having a specified strength of 4000 psi at 28 days was placed and consolidated. Two concrete trucks were needed to place the concrete for all of the panels. Panels 1A to 4A were placed from one truck, while Panels 4B, 5A, and 5B were from the second truck. The concrete mixes contained no admixtures, and had a maximum aggregate size of ¾-inch. Three 4" × 8" concrete cylinders were cast for each

mixture and used for compression testing at the time of the shock tube tests. Tests were completed over a one-week time span, once the panels had cured for 28 day days. The concrete in Panels 1A through 4A had an average compressive strength of 4700 psi, while Panels 4B, 5A and 5B had an average strength of 6800 psi.

Table 4. Reinforced Concrete Panel Test Matrix

Panel	Span L (ft)	Thick T (in)	L/T	ρ (%)	ρ/ρ_b	Stirrups	Objective of Test
1A	8	12	8	0.16	0.06	90°/135° @ $d/2$	Lower bound of L/T and minimum allowed vertical wall steel
1B	8	12	8	0.15	0.06	None	
2A	8	8	12	0.68	0.25	None	Singly reinforced wall (2A) and doubly reinforced (2B) of equal strength
2B	8	8	12	0.24	0.10	None	
3A	12	8	18	0.39	0.16	135°/135° @ $d/2$	Minimum allowed reinforcement for beams
3B	12	8	18	0.37	0.13	None	
4A	12	8	18	0.74	0.31	135°/135° @ $d/2$	Maximum reinforcement to obtain Heavy damage in shock tube, focusing on different stirrup layouts
4B	12	8	18	0.74	0.25	135°/135° @ d	
5A	12	8	18	0.71	0.20	135°/135° @ d on alternating bars	
5B	12	8	18	0.71	0.20	None	

Table 5. Primary Reinforcing Details of Tested Panels

Panel	Primary Reinforcing	f_y (ksi)	f'_c (ksi)	d (in.)	d' (in.)
1A	4 #4 e.f.	72.1	4.7	10.38	1.63
1B	4 #4 e.f.	72.1	4.7	10.75	1.25
2A	4 #5 ctr.	66.4	4.7	4.25	N/A
2B	4 #4 e.f.	72.1	4.7	6.88	1.38
3A	6 #4 e.f.	72.1	4.7	6.38	1.63
3B	4 #5 e.f.	66.4	4.7	6.94	0.94
4A	5 #6 e.f.	74.7	4.7	6.25	1.75
4B	5 #6 e.f.	74.7	6.8	6.25	1.75
5A	7 #5 e.f.	66.4	6.8	6.31	1.69
5B	7 #5 e.f.	66.4	6.8	6.31	1.69

EXPERIMENTAL SETUP

Fig. 3 shows two wall panels, mounted adjacent to one another, in the BakerRisk shock tube. Panel series 1 and 2 had 8 ft spans and were mounted in the 8 ft × 8 ft shock tube. Panel series 3, 4, and 5 had 12 ft spans, and were mounted in the 10 ft × 10 ft shock tube. This prevented a 1 ft length over the top and bottom from being loaded. This produces a maximum moment only 3% less than a similar panel loaded over its entire 12 ft span, which was accounted for in the analysis to follow.

A slight (¼-inch) gap was left between the vertical edges of the panels to prevent any form of panel-to-panel contact. The walls were seated on narrow steel plates, and a gap was provided at the top of the panels to prevent compression membrane action. Panels were mounted vertically and supported laterally along their top and base with horizontal HSS sections that were bolted snug-tight to the shock tube. Load cells were placed between the HSS tubes and rigid boxes, welded to the shock tube, as shown in Fig. 3. Two load cells per panel measured the dynamic reaction histories during each test.

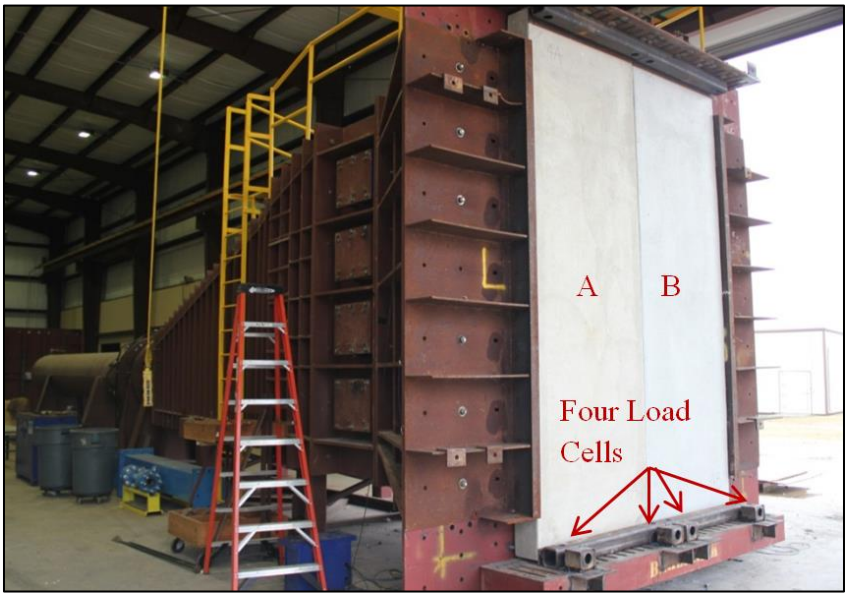

Fig. 3 Wall Specimens Mounted in Shock Tube

Displacements were measured by overlaying a grid on the side-elevation high-speed (HS) video recordings for each panel. Additional HS and high-definition (HD) videos were taken from the front elevation. Photographs were taken before and after each test, and cracks were traced with markers to increase visibility in the photographs.

Whenever possible, multiple (repeat) tests were conducted on the same panels to maximize the amount of data produced from this series. Note that the tests (numbered 1–15) are numbered independently of the panel numbers (1–5).

EXPERIMENTAL RESULTS

Table 6 provides a summary of the experimental data for Test 4 through 15. This includes peak pressure and impulse which characterize the applied load, peak support rotation θ_{max}, residual support rotation θ_{res}, and a qualitative description of damage. Tests 1 through 3 were elastic shots on Panel Series 1 and 2, and are therefore insignificant in this study. For brevity, full test descriptions and observations were not included in this paper. The next subsections focus on key insights gained from the experimental program. Undamaged panels are classified as those with no prior testing exceeding the elastic limit; namely Test 4, Test 6, Test 9, Test 12 and Test 13.

Effect of Shear Stirrups

Doubly reinforced panels with similar vertical reinforcement ratios but different levels of shear stirrups were studied in the test series. Peak support rotations ranging from 2° to 16° showed no marked difference between panel performances due to the presence of shear reinforcement. Differences in the displacements were typically attributed to different material strengths and difference in concrete cover, as listed in Table 5. Panels with shear stirrups kept the core concrete confined, and spalling was limited to the cover concrete (Fig. 4(a)). In contrast, members without shear stirrups showed signs of crushing beyond the compression face steel (Fig. 4(b)) with increased support rotations. The loss of core concrete will adversely decrease the static strength and stiffness of panels after a blast event. Shear cracks were not observed on panels without shear reinforcing (1B, 2A, 2B, 3B, and 5B), although conventional shear stress capacities were exceeded.

(a) Panel 3A – Stirrups at *d*/2 (b) Panel 3B – No shear stirrups

Fig. 4 Compression Face Damage - Test 11

Table 6. Experimental Results

Test	P (psi)	i (psi-ms)	Panel	θ_{max}	θ_{res}	Damage
4[a]	14.9	320	2A	2.1°	0.3°	1 mm maximum tension cracks
			2B	1.5°	0.6°	1 mm maximum tension cracks, onset of concrete crushing on compression face
5[b]	15.2	405	2A	7.7°	3.3°	Crushing extended to vertical steel (mid-depth)
			2B	3.0°	1.8°	No crushing on compressive face
6[a]	20.0	900	1A	3.3°	2.4°	5.5 mm maximum tension cracks
			1B	2.7°	1.8°	6.5 mm maximum tension cracks
7[b]	20.8	1215	1A	5.1°	4.2°	Crushing on compression face over 3-inch tall strip at mid-height
			1B	4.2°	3.3°	No crushing on compression face
8[b]	19.9	1250	1A	Blowout		Fracture of vertical steel at 9.8° support rotation
			1B	Blowout		Failure of wall
9	11.5	570	3A	5.4°	3.2°	4 mm maximum tension cracks, no crushing on compression face
			3B	5.9°	3.8°	4 mm maximum tension cracks, no crushing on compression face
10[b]	11.8	305	3A	6.9°	5.4°	Crushing on compression face, spalling to depth of stirrups
			3B	6.9°	4.6°	No crushing on compression face
11[b]	11.5	300	3A	10.4°	7.9°	Crushing over a 30-inch height at mid-span on compression face
			3B	8.4°	6.3°	Crushing over a 12-inch height at mid-span on compression face
12	18.5	1050	4A	16.3°	11.8°	Non-uniform crushing over a 48-inch height at mid-span on compression face
			4B	14.8°	10.8°	Crushing over a 48-inch height at mid-span on compression face
13	14.8	590	5A	3.2°	1.2°	No crushing on compression face
			5B	3.2°	1.2°	No crushing on compression face
14[b]	15.6	720	5A	9.5°	6.9°	Crushing over a 36-inch height at mid-span on compression face
			5B	7.7°	5.6°	Crushing over an 8-inch height at mid-span
15[b]	15.6	720	5A	N/A[c]	11.6°	Crushing over a 56-inch height at mid-span on compression face, restricted to cover concrete
			5B	N/A[c]	9.5°	Crushing over a 56-inch height at mid-span on compression face, de-bonding between compression bars and core concrete

[a] Re-test of undamaged panel; previous tests were elastic, with no tensile cracking observed
[b] Re-test of damaged panel; support rotations reported are cumulative
[c] Peak displacement not obtained; residual displacement tabulated

Experimental Support Rotations at Crushing

Fig. 5 plots the peak support rotation for each panel as a function of the tensile steel percentage as well as the ratio of actual to balanced steel ratio; the plots distinguish tests where crushing occurred (red dots) from those in which no crushing was observed (blue). The plots do not distinguish between the different *L/T* ratios, as the data set is not large enough. The graphs can be summarized by the following key points:

- The sole single-reinforced panel tested experienced crushing at just over 2° support rotation.
- The lowest support rotation at which a doubly-reinforced panel experienced crushing was 5°, well above the currently accepted criterion of 2°. Non-crushing panels were observed out to 7°, suggesting a range of 5–7° for the onset of crushing.
- The points plotted include both panels with stirrups as well as those without; no indication was observed suggesting that panels with stirrups are able to tolerate a larger rotation prior to crushing.
- One panel with *L/T* = 8, and a reinforcing ratio of approximately 0.15% experienced crushing at 5°. However, panels with higher reinforcing contents of 0.33% did not have crushing until 7°. This was on the 12-ft panels that had *L/T* = 18. The onset of crushing is a factor of both reinforcing content and span-to-thickness ratio, which was supported by the analytical model that follows.

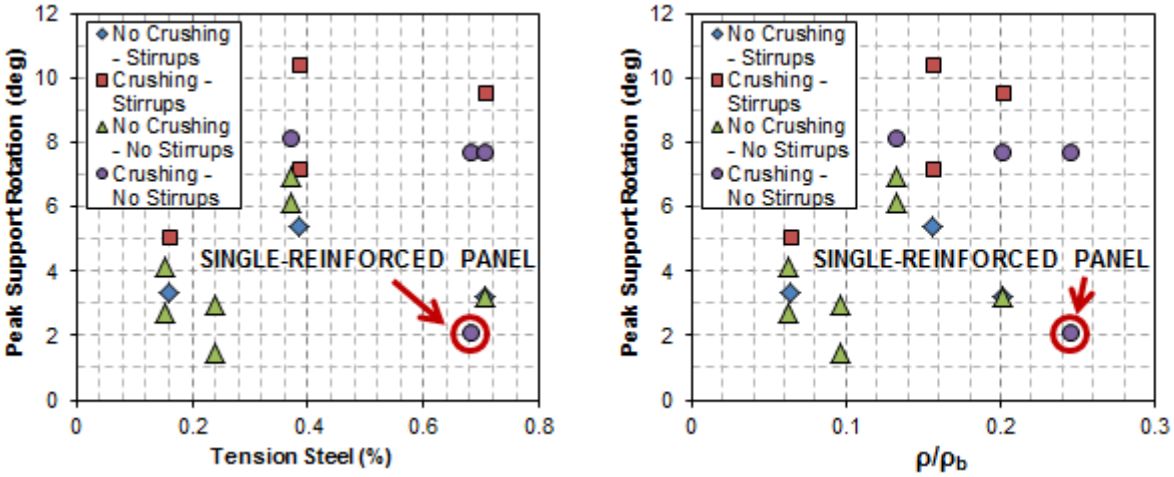

Fig. 5 Experimental Crushing at Support Rotations

Peak and Residual Support Rotations

Fig. 6(a) plots the experimentally measured peak and residual support rotations for the panels tested in an undamaged state, i.e., first-time tests on a given panel (Tests 4, 9, 12, and 13). All of the panels, both initial tests and retests, are plotted in Fig. 6(b). Linear trendlines were added to both plots, with equations for residual support rotation as a function of peak support rotation shown. The equations are approximately the same, indicating that residual support

rotations are independent of prior loading history. The trendlines show an increasing difference between peak and residual support rotations with increasing maximum support rotations.

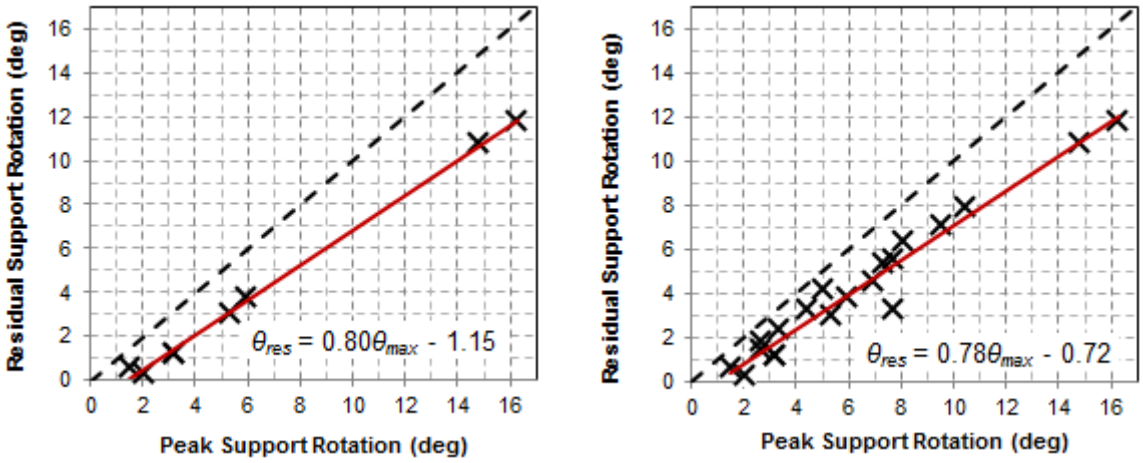

(a) Undamaged Panels (b) All Panels

Fig. 6 Experimental Peak vs. Residual Displacement

ANALYSIS OF TEST RESULTS

The analytical methods presented earlier in this paper were used to model the experimental tests performed. Single-degree-of-freedom (SDOF) resistance curves were derived using three different models, as follows:

(1) Elastic-plastic with default static increase factors (SIFs) for concrete and steel.
(2) Elastic-plastic with concrete and steel strengths measured from material testing.
(3) Multi-linear model from moment-curvature, using measured material property strengths.

Note that the elastic-plastic resistance functions do not consider concrete crushing or a subsequent drop in moment capacity at 2 degrees, as recommended in PDC TR-06-08. Had this been considered, predicted displacements would have increased beyond the values reported in this paper. Dynamic increase factors (DIFs) were taken as the default recommended values from blast guidelines for both models (1) and (2). For model (3), calculations were iterated to find the actual strain rates of steel and concrete, and the corresponding value of DIF obtained from published curves available in UFC 3-340-02. This is possible with such a model, as the strains are known within a cross section at any level of displacement. It was found from all of the analyses performed that the default DIFs were within 5–10% accuracy of the actual DIFs calculated with the moment-curvature model.

Analyses on both panels were performed for Test 4 through Test 15. Tests 1 through 3 were omitted as their displacements were minimal. A total of twelve tests, with two panels in each test, were analyzed with the three analytical methods above. This resulted in 72 individual

SDOF analyses. For each test, the peak displacement, residual displacement, and dynamic reactions were of particular interest.

PEAK AND PERMANENT DISPLACEMENTS

Results for undamaged panels are presented, followed by comparisons for panels tested multiple times. Undamaged panels are classified as those with no prior testing exceeding the elastic limit, namely Test 4, Test 6, Test 9, Test 12, and Test 13. Computed and experimental peak permanent support rotations are plotted in Fig. 7(a) and (b), respectively. Ratios of predicted-to-measured peak and permanent displacements are plotted in Fig. 7(c) and (d), respectively. Ratios greater than unity imply design-conservative peak displacement predictions (i.e., model over-predicts displacement).

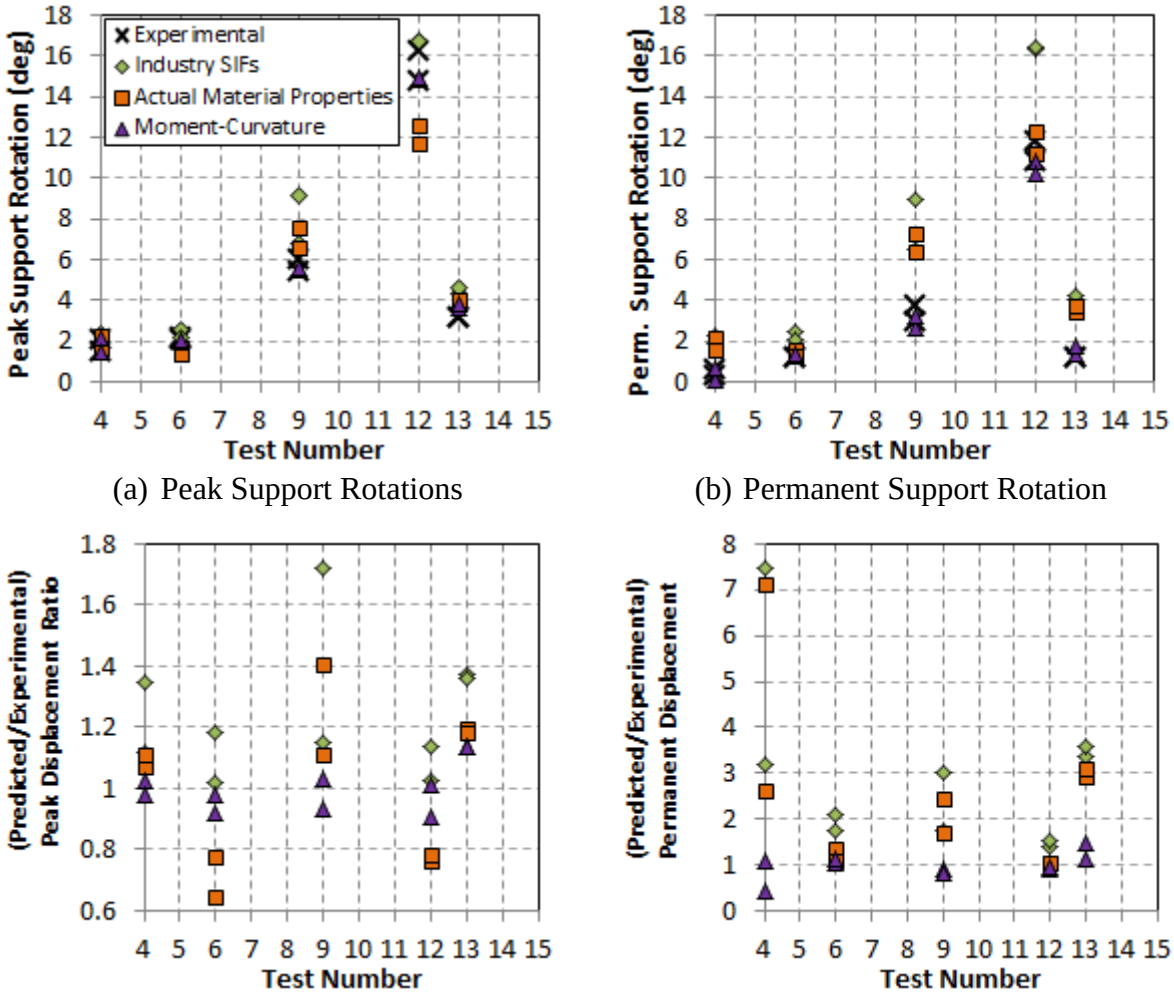

(a) Peak Support Rotations (b) Permanent Support Rotation

(c) Ratio of Peak Displacements (d) Ratio of Permanent Displacements

Fig. 7 Support Rotations and Prediction Ratios for Undamaged Panels

These plots show that typical SDOF modeling approaches used in design (Model (1)) are conservative in predicting peak displacements. This conservatism was reduced when using

the actual material properties of the concrete and steel (Model (2)), which tended to be higher than the assumed SIFs. Test 9 is important to note, as the actual support rotations (less than 6°) would still satisfy a Heavy damage limit. However, using default SIFs, typical SDOF over-predicts the peak displacement by a factor of 1.8, leading to a belief that the panel would have failed when using empirical criteria.

Moment-curvature predictions provide a higher order of accuracy for peak displacement predictions. The predicted displacements are, however, slightly non-conservative in some cases, but within 10% accuracy. More important, however, is the superior accuracy of permanent displacement predictions. Fig. 7(d) shows over-estimates of permanent displacement typically on the order of 2 to 3, for elastic-plastic SDOF analyses. The outlying case with an over-estimate ratio of about 7 is for the singly reinforced Panel 2A, which had a very small permanent displacement of ½-inch. Hence the relative difference is less significant than it appears.

Fig. 8 combines the ratios of peak and permanent analytical predictions to experimental measurements for all undamaged panel tests. The vertical axis represents the peak displacement ratio, and the horizontal axis the permanent displacement ratio. Scatter is reduced, particularly with permanent displacement predictions when using the multi-linear moment-curvature model. Peak displacements were within 10% accuracy of measured values, and typically with 10% accuracy for the permanent displacements as well. The two outlying cases were for small deflections, where the predicted displacements were within ½-inch of one another.

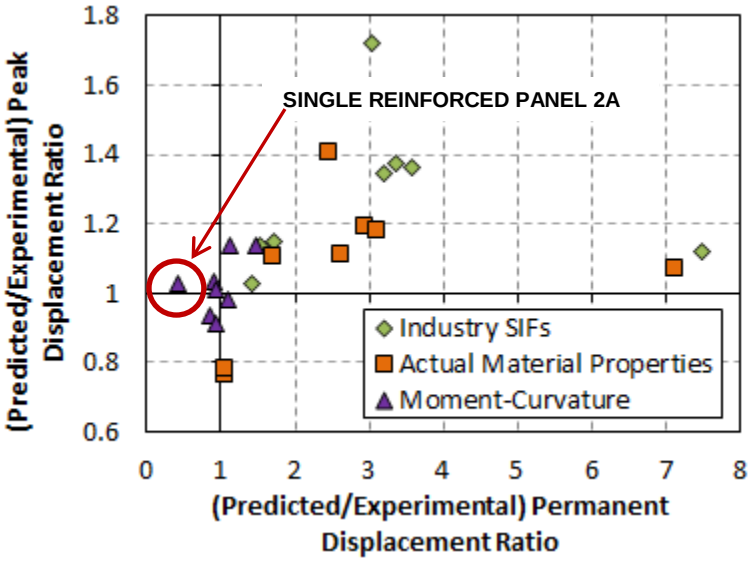

Fig. 8 Analytical Predictions for Undamaged Panels

In practice, SDOF analyses are usually performed on undamaged components. However, there are instances where multiple shock loads may occur subsequently, such as in containment enclosures with inadequate venting, or from bursting pressure vessels.[15] Elastic-plastic resistance functions used in typical SDOF assume the same unloading and re-loading

stiffness. In contrast, the moment-curvature models follow the Takeda hysteretic rules described in this paper, accounting for reloading stiffness in repeated tests.

Example displacement histories for Panel 3A, which was tested three times, are plotted in Fig. 9. The vertical axis is the individual displacement for each test, with the total displacement requiring the addition of the previous permanent displacement. These curves demonstrate the ability for both peak and residual displacements to be accurately predicted using a moment-curvature model with modified Takeda unloading. This adjustment of stiffness throughout the panel response accurately models the natural period elongation that is observed in experimental tests.

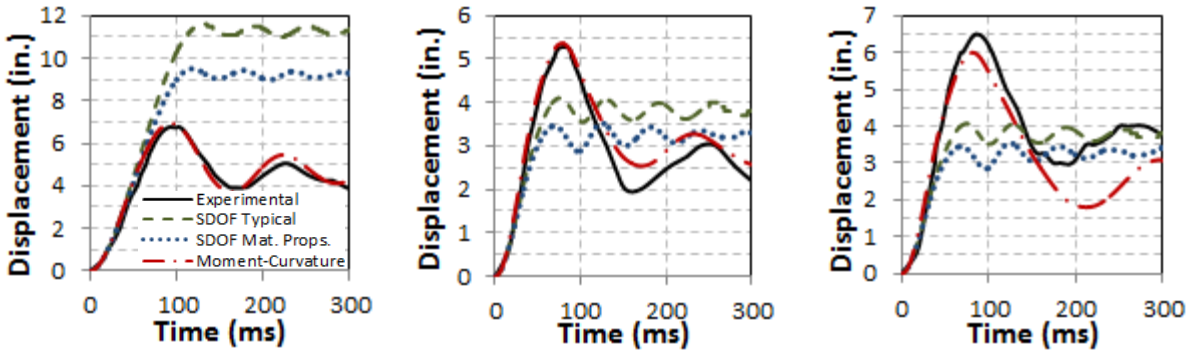

(a) Test 9 (b) Test 10 (c) Test 11

Fig. 9 Repeated Testing of Panel 3A

Fig. 10 plots the ratios of predicted-to-experimental peak and permanent displacements for all tests. Data is not provided for Test 8, as both panels failed. The hysteretic model used with the moment-curvature resistance predicted peak displacements (Fig. 10(a)) to be within 20% of experimental displacements. Elastic-plastic methods provided poor predictions of peak displacement in repeat tests, and were neither consistently conservative nor non-conservative. Similar trends were seen in the prediction of permanent displacements (Fig. 10(b)).

DYNAMIC SUPPORT REACTIONS

Dynamic support reactions were measured for panels in each test. Analytical dynamic reactions were calculated using standard coefficients specified[4] for simply-supported, uniformly loaded panels. Experimental values tended to be higher than the calculated values, as shown in the plot of Fig. 11(a) for the undamaged panels. Note that in these plots, a value lower than 1.0 would be non-conservative; as it indicates a predicted force lower than the measured force. Fig. 11(b) plots an experimentally measured reaction history against the three analytical model predictions. This illustrates the benefit of using a more refined moment-curvature model over elastic-plastic methods. The duration of reactions following the first inbound phase are more representative of the measured values, and rebound reactions, which are important in the design of precast connections, are greatly reduced.

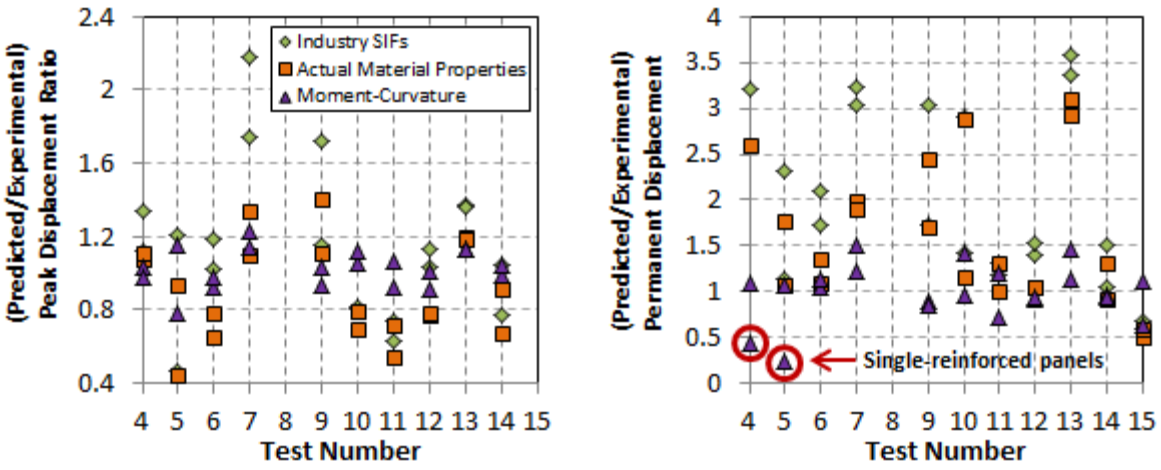

(a) Ratio of Peak Displacements (b) Ratio of Permanent Displacements

Fig. 10 Peak and Residual Displacement Ratios for All Panels

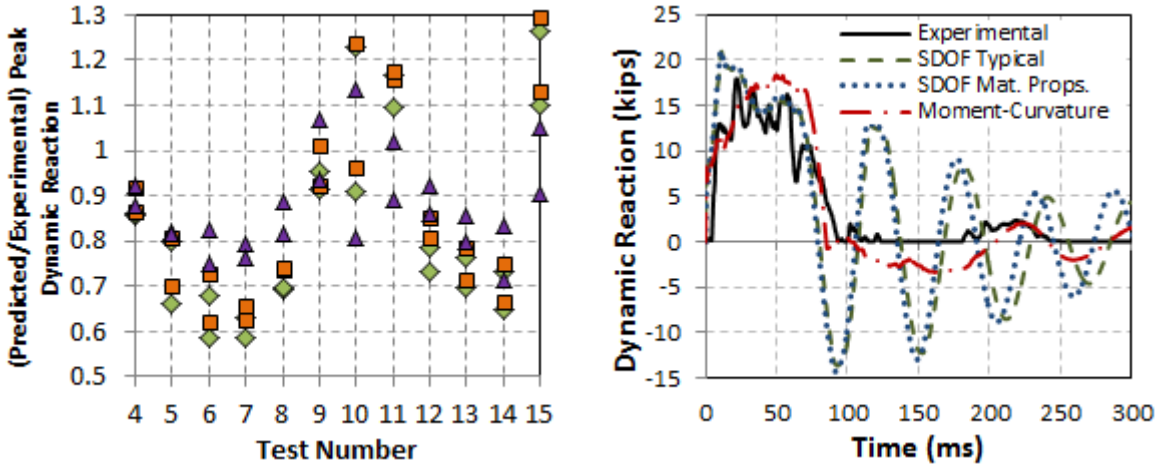

(a) All Panel Accuracy Ratios (b) Dynamic Reactions: Test 11 (3B)

Fig. 11 Experimental and Analytical Peak Dynamic Reaction Comparisons

DESIGN EXAMPLE

This section demonstrates the use of qualitative response criteria with moment-curvature resistance functions. Consider a new building design with an inter-story height of 14 ft and non-load bearing concrete wall façade with a maximum thickness of 6 inches. The blast specification requires a Moderate response design threat of 30 psi, 180 psi-ms. Using an elastic-plastic resistance function, and a quantitative 2° maximum support rotation, the panel reinforcement is designed. Using ASTM615 Gr. 60 steel and 5000 psi concrete, it is determined that a reinforcement ratio of 1.1% (ρ/ρ_b = 0.52) on both faces is needed. The peak SDOF displacement is calculated to be 2.9 inches (2°). The residual displacement is calculated to be 1.8 inches at mid-span.

The panel is now designed for a Moderate response, using qualitative response criteria. From

Table 3, this would correspond to spalling of the cover concrete with the core concrete having minor damage. From a moment-curvature analysis, it is determined that the reinforcement ratio can be reduced to 0.5% ($\rho/\rho_b = 0.23$), less than half of the previous value. This reduces the resistance of the panel significantly (Fig. 12(a)). However, it is anticipated from the model that the onset of crushing will occur at approximately 5.8 degrees support rotation (8.5-inch displacement). Under the given loading, the peak displacement of the panel is 5.6 inches (3.8°), providing some reserve before spalling would be observed. The residual displacement is calculated to be 1.3 inches. The initial peak dynamic reaction is the same for both panels (governed by the blast load), but lasts for less than 10 ms before reaching the equivalent static load (Fig. 12(d)). The inbound reaction for this panel is approximately half of the elastic-plastic design, and for rebound, approximately one-third.

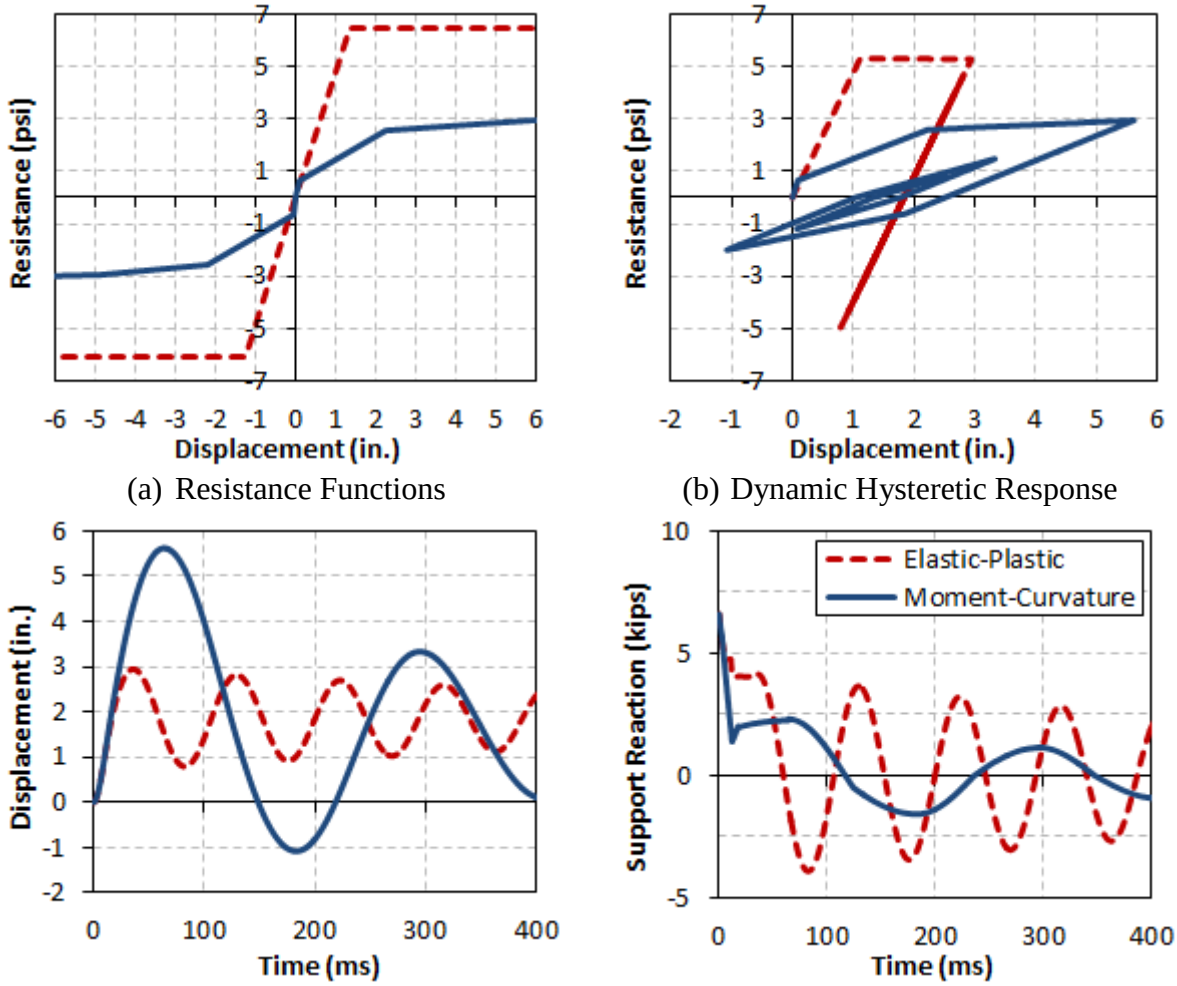

(a) Resistance Functions (b) Dynamic Hysteretic Response

(c) Displacement Predictions (d) Dynamic Reactions

Fig. 12. Design Example Using Different SDOF Resistance Functions

CONCLUSIONS

Based on the literature review, experimental study, and analytical findings presented in this report, the following conclusions can be made:

1. A full-scale shock tube test program demonstrated that non-load bearing double-reinforced concrete walls can deflect significantly higher than prescribed blast design limits. For the panels tested, a 5–7° rotation criterion is more indicative of the onset of crushing (which corresponds to the upper bound of Moderate damage) than the traditional 2°.
2. For single-reinforced panels, the traditional 2° criterion for Moderate damage was confirmed as being appropriate.
3. Panels tested were governed by flexural response, with shear reinforcement provided near the ends of Panels 4B and 5B to ensure this. No appreciable difference in rotation at the onset of crushing was observed between panels with or without stirrups in the experimental program.
4. A multi-linear resistance function derived through a moment-curvature analysis allows for more accurate (and less conservative) predictions of panel displacement and rotation than currently used typical elastic-plastic idealization. With such a model, structural blast engineers can design to qualitative damage limits, rather than to current empirical quantitative response limits. The qualitative limits of ASCE 59-11 provide reasonable qualitative damage expectations to the concrete cover, core and steel reinforcement.
5. The moment-curvature model is significantly more reliable at predicting residual displacements than the elastic-plastic model. This is of less concern for design, but can be important in load-bearing walls, blast loads with a significant negative phase, and in post-damage assessments, such as for accident reconstructions, when only residual displacements are available.

The above conclusions are applicable to panels within the parameter limits imposed on the current study, namely:

- One-way, non-load-bearing, conventionally reinforced panels
- L/T ratio between 8 and 18 (thus, flexural response dominates over shear response)
- Walls not requiring stirrups for shear stress resistance
- Normal strength concrete (nominally 4,000 psi) and rebar (nominally 60 ksi)
- Relatively light primary reinforcement ($< 0.25\rho_b$)

Response limits that are all encompassing for typical panel geometries and reinforcement contents can be derived using analytical models similar to those presented.

ACKNOWLEDGMENTS

This work was funded by the Explosion Research Cooperative (ERC), a joint-industry program led by BakerRisk, with 21 participants from the refining and petroleum industries. The ERC has been established since 1993, researching blast effects and their impacts on

buildings, equipment, and personnel. Additional funding was provided by BakerRisk through Internal Research initiatives.

REFERENCES

1. ACI Committee 318, *Building Code Requirements for Structural Concrete (ACI 318-08) and Commentary (ACI 318-08R)*, Farmington Hills, Michigan, 2008.
2. PCI Industry Handbook Committee, *PCI Design Handbook – Precast and Prestressed Concrete*, Seventh Edition, Chicago, Illinois, 2010.
3. ASCE 59-11, *Blast Protection of Buildings*, Published by the American Society of Engineers (ASCE), Reston, VA, 2011.
4. PDC TR-06-01, "Methodology Manual for the Single-Degree-of-Freedom Blast Effects Design Spreadsheets (SBEDS)," U.S. Army Corps of Engineers (USACE), Protective Design Center (PDC) *Technical Report 06-01*, Sep. 2006.
5. PDC TR-06-08, "Single Degree of Freedom Response Limits for Antiterrorism Design," USACE PDC *Technical Report 06-08*, Jan. 2008.
6. PDC TR-08-07, "Methodology Manual for Component Explosive Damage Assessment Workbook (CEDAW)," USACE PDC, *Technical Report 08-07*, Sep. 2008.
7. Forsen, R., "Airblast Loading of Wall Panels," Swedish National Defense Research Institute, *FOA Report C 20586-D6*, October 1985.
8. Coltharp, D.R., Vitayaudom, K.P., and Kiger, S.A., "Semihardened Facility Design Criteria Improvement," U.S. Army Waterways Experiment Station for Engineering and Services Laboratory at Tyndall AFB, *Report No. ESL-TR-85-32*, Sep., 1985.
9. Wright, S.J., "Scaled Testing and Analysis of Concrete Buildings and Components," Naval Air Warfare Center Weapons Division, *Report No. NAWCWPNS TM 7554*, April, 1993.
10. Karthik, M.M., and Mander, J.B. (2011). "Stress-Block Parameters for Unconfined and Confined Concrete Based on a Unified Stress-Strain Model," *Journal of Structural Engineering*, Vol. 137, No. 2, Feb. 2011, pp. 270-273.
11. Mander, J.B., Priestley, M.J.N., and Park, R. (1988). "Theoretical Stress-Strain Model for Confined Concrete," *Journal of Structural Engineering*, Vol. 114, No. 8, Aug. 1988, pp. 1804-1826.
12. Malvar, L.J. (1998). "Review of Static and Dynamic Properties of Steel Reinforcing Bars," *ACI Materials Journal*, Vol. 95, No. 5, Sep.-Oct. 1998, pp. 609-614
13. Keenan, W.A, "Blast Loading of Concrete Beams Reinforced With High-Strength Deformed Bars," U.S. Naval Civil Engineering Laboratory, Port Hueneme, California, *Technical Report R-226*, Apr. 1963.
14. Takeda, T., Sozen, M., A., and Nielsen, N.N. (1970). "Reinforced Concrete Response to Simulated Earthquakes," *Journal of the Structural Division*, Proceedings of the ASCE, Vol. 96, No. ST 12, Dec. 1970, pp. 2557-2573.
15. Baker, W.E., Cox, P.A., Westine, P.S., Kulesz, J.J., and Strehlow, R.A., *Explosion Hazards and Evaluation*, Elsevier Scientific Publishing Company, New York, NY, 1983.